research papers

Lattice parameters and structural phase transition of lanthanum titanate perovskite, $La_{0.68}(Ti_{0.95},Al_{0.05})O_3$

Roushown Ali and Masatomo Yashima*

Department of Materials Science and Engineering, Interdisciplinary Graduate School of Science and Engineering, Tokyo Institute of Technology, 4259 Nagatsuta-cho, Midori-ku, Yokohama 226-8502, Japan.
E-mail: yashima@materia.titech.ac.jp

Lattice parameters and the structural phase transition of $La_{0.68}(Ti_{0.95},Al_{0.05})O_3$ have been investigated *in situ* in the temperature range 301–689 K by the synchrotron radiation powder diffraction (SR-PD) technique. High-angular-resolution SR-PD is confirmed to be a powerful technique for determining precise lattice parameters around a phase-transition temperature. The title compound exhibits a reversible phase transition between orthorhombic and tetragonal phases at 622.3 ± 0.6 K. The following results were obtained: (i) the lattice parameters increased continuously with temperature, while the b/a ratio decreased continuously with temperature and became unity at the orthorhombic–tetragonal transition point; (ii) no hysteresis was observed between the lattice-parameter values measured on heating and on cooling. Results (i) and (ii) indicate that the orthorhombic–tetragonal phase transition is continuous and reversible. The b/a ratio is found to exhibit a more continuous temperature evolution than does the order parameter for a typical second-order phase transition based on Landau theory.

1. Introduction

$La_{2/3}TiO_3$-based compounds with an *A*-site deficient perovskite-type structure exhibit interesting electrical, dielectric and magnetic properties (Yokoyama *et al.*, 1989; Yoshioka, 1994; Kim *et al.*, 1994; MacEachern *et al.*, 1994; Yoshioka & Kikkawa, 1998; Suvorov *et al.*, 1998). This structure can be stabilized either by doping a metal oxide, such as Al_2O_3 (Skapin *et al.*, 1993; Yoshioka & Kikkawa, 1998; Yashima *et al.*, 2000; Ali *et al.*, 2001) or Nb_2O_5 (Ali *et al.*, 2002; Yoshioka, 2002), into $La_{2/3}TiO_3$ or by heating $La_{2/3}TiO_{3-\delta}$ under a reducing atmosphere (Yokoyama *et al.*, 1989; Kim *et al.*, 1994). $La_{0.68}(Ti_{0.95},Al_{0.05})O_3$ has a double perovskite-type structure along the *c* axis and exhibits a structural phase transition from low-temperature orthorhombic to high-temperature tetragonal phase between 473 and 673 K (Yashima *et al.*, 2000; Ali *et al.*, 2001). Yoshioka & Kikkawa (1998) investigated electrical properties of $La_{(2+x)/3}(Ti_{1-x},Al_x)O_3$ and reported that $La_{0.68}(Ti_{0.95},Al_{0.05})O_3$ ($x = 0.05$) has the highest bulk ionic conductivity in the compounds with $x = 0.05$–0.20. Because of the high ionic conductivity, this compound can be used as a component of solid oxide fuel cells (SOFCs). Thermal expansion and the temperature dependence of the lattice parameters are important factors in designing components of SOFCs (Yashima *et al.*, 2000). Therefore, we studied the orthorhombic–tetragonal phase transition of $La_{0.68}(Ti_{0.95},Al_{0.05})O_3$ with conventional laboratory-based X-ray diffractometers (Yashima *et al.*, 2000; Ali *et al.*, 2001) but found it very difficult to determine precise lattice parameters around the transition point. Synchrotron radiation

powder diffraction (SR-PD), however, is a very useful technique for the determintion of precise lattice parameters and the investigation of phase changes (Hart *et al.*, 1990; Yashima *et al.*, 1998; Yashima *et al.*, 2001; Ali *et al.*, 2002). The conventional X-ray diffractometry usually produces broad diffraction peaks with asymmetric shape and yields double peaks ($K\alpha_1$ and $K\alpha_2$) for one reflection, leading to a complicated peak profile. On the contrary, the SR-PD yields only a single peak for one reflection. Furthermore, an SR-PD peak can be much narrower and has a relatively symmetric shape. As reported in earlier studies (Yashima *et al.*, 2000; Ali *et al.*, 2001), there is very little difference between the lattice parameters *a* and *b* around the orthorhombic–tetragonal phase-transition point. Thus, the separation of the 020 and 200 peaks was almost impossible using conventional X-ray diffraction.

The purpose of this study is (i) to measure precisely the lattice parameters of $La_{0.68}(Ti_{0.95},Al_{0.05})O_3$ as a function of temperature and (ii) to determine accurately the phase-transition temperature of the compound *via* the high-resolution synchrotron radiation X-ray powder diffraction technique. The temperature evolution of the axial ratio *b/a* is discussed in relation to Landau theory.

2. Experimental

$La_{0.68}(Ti_{0.95},Al_{0.05})O_3$ was prepared by solid-state reactions at 1673 K. Details of the synthesis are described elsewhere (Yashima *et al.*, 2000; Ali *et al.*, 2001).

To determine precisely the temperature dependence of the lattice parameters, high-resolution SR-PD experiments were conducted on beamline BL-3A (Sasaki *et al.*, 1992; Kawasaki *et al.*, 1992; Ali *et al.*, 2002) at the Photon Factory, High Energy Accelerator Research Organization (KEK), Tsukuba, Japan. An incident beam of wavelength 1.37852 (6) Å from an Si(111) double-crystal monochromator was used. A configuration in which the X-rays diffracted from the sample powder are diffracted again by an Si(111) analyzer crystal before reaching the detector was used, in order to improve the angular resolution as much as possible (Stephens *et al.*, 2002). Data were collected from the sample powders in an asymmetric flat-plate reflection geometry, in air, in the temperature range 301–689 K. A small furnace (Tanaka, 2000; Ali *et al.*, 2002) with Fe–Cr heaters was attached to a goniometer of the triple-axis/four-circle diffractometer (Kawasaki *et al.*, 1992) and used for SR-PD measurements at high temperatures. The sample temperature was kept constant within ± 0.5 K during each measurement. The wavelength was determined by the calibration method described below (Ali *et al.*, 2002). The profiles of eight reflections of a standard NIST CeO_2 sample (a = 5.41129 Å) were obtained by a step-scanned technique, and the exact peak positions, $2\theta_{obs}$, were calculated with the split-type Pearson VII function and an individual profile-fitting program (*PROFIT*; Toraya, 1986). The peak positions were plotted against *d*-spacing values determined from the lattice parameter a = 5.41129 Å. Then the wavelength, λ, and the zero-point shift, $\Delta\theta$, were estimated with Bragg's equation,

$$\lambda = 2d \sin(\theta_{obs} + \Delta\theta),$$

through a least-squares method.

We measured the peak profile around the 004, 020 and 200 reflections of the orthorhombic phase, because these peaks were the most useful in determining the lattice parameters near the transition point during a short period. To obtain as many data as possible with different temperatures, we measured only the significant 004, 020 and 200 reflections within the limited machine time. The data were collected by scanning only 2θ, where θ was kept at 22.6°. Scanning

parameters were as follows: step interval = 0.004°, counting time = 8 s, diffraction angle 2θ range = 40.80–41.85°, and temperature range = 301–689 K on heating and 344–667 K on cooling. We calibrated the $2\theta_{obs}$ values of the high-temperature SR-PD data by using a zero-point shift, ΔT, which was determined from the SR-PD peak positions measured at room temperature and the lattice parameters obtained from a Rietveld analysis of the same sample (Yashima *et al.*, 2000):

$$a = 3.85933\,(4),\; b = 3.87039\,(4), \quad (1)$$
$$c = 7.77576\,(8)\,\text{Å}.$$

At high temperatures, the lattice parameters were calculated after calibrating the peak position value $2\theta_{obs}$ of the SR-PD data as $2\theta_{obs} - \Delta T$.

3. Results and discussion

3.1. Comparison between the synchrotron radiation and conventional X-ray diffraction data measured at a temperature near the transition point

Fig. 1(*a*) shows the SR-PD profile around the 004, 020 and 200 reflection peaks of $La_{0.68}(Ti_{0.95},Al_{0.05})O_3$, measured at 463 K, and Fig. 1(*b*) shows the conventional X-ray powder diffraction profile obtained at the same temperature. Fig. 1 indicates that SR-PD is much more powerful than conventional X-ray diffraction for distinguishing the 020 peak from the 200 reflection. The refined profile
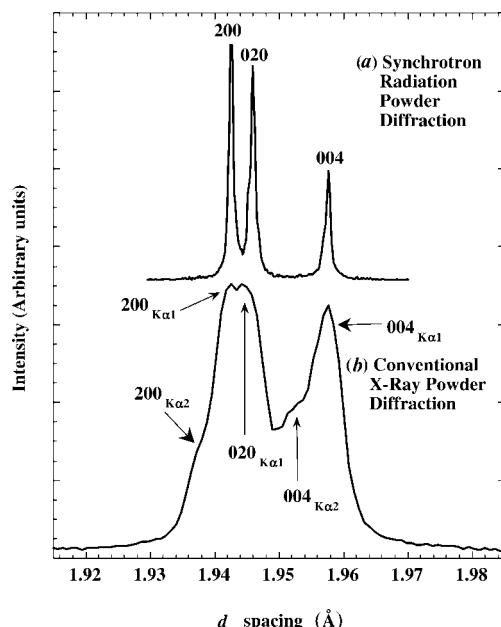
Table 1
Refined parameters of the reflection peak profile of $La_{0.68}(Ti_{0.95},Al_{0.05})O_3$, measured at 463 K with SR-PD and conventional X-ray powder diffraction.

All of the profile parameters are defined by Toraya (1986).

Parameters	Synchrotron radiation			Laboratory X-ray source		
hkl	004	020	200	004	020	200
Integrated intensity (counts × °)	0.54 (1)	1.02 (2)	0.95 (2)	13.5 (3)	9.5 (2)	9.5 (2)
Peak maximum position in 2θ (°)	41.1712 (5)	41.4301 (4)	41.5067 (4)	46.341 (2)	46.640 (4)	46.725 (3)
FWHM, W (°)	0.0217 (7)	0.0209 (6)	0.0182 (5)	0.119 (4)	0.119 (5)	0.119 (5)
Asymmetry, A, defined by W_l/W_h	0.60 (5)	0.76 (6)	1.08 (8)	1.13 (2)	1.5 (1)	1.5 (1)
Decay rate on low-angle side, R_l/η_l	0.96 (3)	0.96 (3)	0.96 (3)	1.51 (9)	1.51 (9)	1.51 (9)
Decay rate on high-angle side, R_h/η_h	1.08 (4)	1.08 (4)	1.08 (4)	1.23 (7)	1.23 (7)	1.23 (7)
2θ range for fitting (°)	40.9–41.8			45.0–47.5		
Step width in 2θ (°)	0.004			0.02		
Scanning time per step (s)	8			1		
Background parameters, b_0	0.30 (2)			2.12 (6)		
Pattern R factor, R_p	0.0961			0.0454		
Pattern weighted R factor, R_{wp}	0.1194			0.0624		
Peak R factor, $R_{p(peak)}$	0.1064			0.0528		
a, b, c (Å)	3.86661 (4), 3.87340 (4), 7.79303 (5)			3.8664 (2), 3.8730 (3), 7.7929 (2)		

parameters of $La_{0.68}(Ti_{0.95},Al_{0.05})O_3$ that are obtained from these diffraction profiles are listed in Table 1. The SR-PD peaks had both a narrower peak width and a more symmetric profile shape than the conventional X-ray powder diffraction peaks. In fact, the FWHM, W, of the SR-PD peaks had values ranging from 0.0182 to 0.0217°, while the conventional X-ray powder diffraction peaks had much larger W values of 0.119° (Table 1). The refined asymmetry parameters, A, for the SR-PD profile were in the range 0.60–1.08, while the A parameters for the conventional X-ray powder diffraction peaks were 1.13–1.5. Furthermore, SR-PD did not yield any doublet but only a single peak for one reflection, although there was a $K\alpha_1$ and $K\alpha_2$ doublet for one reflection in the conventional X-ray diffraction profile (Fig. 1). Therefore, SR-PD enabled a more precise determination of the reflection peak positions than the conventional X-ray technique. For example, at 463 K, the peak position for the 020 reflection was estimated to be 46.640 (4)° by conventional X-ray powder diffraction, while the SR-PD data gave the peak position at 41.4301°, with a higher precision of ±0.0004° at the same temperature. Thus, SR-PD enabled the determination of higher-precision lattice parameters at 463 K, *viz.*

$$a = 3.86661\,(4),\; b = 3.87340\,(4),\; c = 7.79303\,(5)\,\text{Å},$$

compared with the values

$$a = 3.8664\,(2),\; b = 3.8730\,(3),\; c = 7.7929\,(2)\,\text{Å},$$

which were obtained at the same temperature by conventional X-ray diffraction.

These results indicate that SR-PD can more precisely determine the peak positions and lattice parameters near a phase-transition point. Similarly precise lattice parameters were obtained over the whole temperature range, as shown in Table 2. The precision of the lattice parameters ranged from ±0.00002 to ±0.00007 Å except for the data obained at 622 K. The estimated standard deviation for the lattice parameters a, b and $c/2$, which were used to determine the zero-point shift ΔT, was $\sigma = \pm0.00004$ Å, as shown in (1). Thus, the accuracy of the lattice parameters might be approximately $3\sigma = \pm0.00012$ Å.

Figure 1
(*a*) Synchrotron and (*b*) conventional X-ray powder diffraction profiles of the 004, 020 and 200 reflection peaks of $La_{0.68}(Ti_{0.95},Al_{0.05})O_3$, measured at ~463 K. The lattice spacing (*d* value in the horizontal axis) was calculated from 2θ with Bragg's equation, $\lambda = 2d\sin\theta$. The values $\lambda = 1.54056$ and $\lambda = 1.37852\,(6)$ Å were used for the conventional and synchrotron data, respectively.

Table 2
Lattice parameters and unit-cell volume of $La_{0.68}(Ti_{0.95},Al_{0.05})O_3$ as a function of temperature.

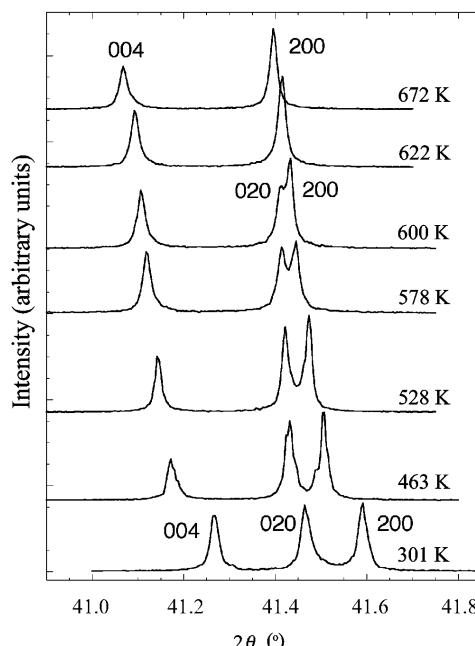| Temperature (K)	a (Å)	b (Å)	c (Å)	V (Å³)
Heating				
301	3.85913 (4)	3.87046 (4)	7.77601 (7)	116.147 (3)
378	3.86302 (3)	3.87216 (3)	7.78484 (5)	116.447 (2)
411	3.86440 (4)	3.87246 (4)	7.78786 (7)	116.543 (3)
443	3.86591 (3)	3.87303 (2)	7.79035 (5)	116.643 (2)
463	3.86661 (4)	3.87340 (4)	7.79303 (5)	116.716 (3)
484	3.86772 (3)	3.87365 (3)	7.79402 (5)	116.772 (2)
504	3.86860 (3)	3.87394 (3)	7.79632 (9)	116.841 (3)
514	3.86923 (3)	3.87411 (3)	7.79729 (7)	116.880 (3)
523	3.86964 (2)	3.87427 (2)	7.79758 (4)	116.902 (2)
528	3.86981 (3)	3.87428 (2)	7.79794 (9)	116.912 (3)
532	3.86980 (2)	3.87447 (2)	7.79861 (4)	116.928 (2)
537	3.87012 (2)	3.87444 (2)	7.79909 (5)	116.944 (2)
542	3.87042 (2)	3.87443 (2)	7.79929 (7)	116.956 (2)
547	3.87067 (2)	3.87452 (2)	7.79989 (5)	116.975 (2)
551	3.87089 (2)	3.87460 (2)	7.80037 (4)	116.991 (2)
556	3.87107 (3)	3.87462 (2)	7.80075 (5)	117.003 (2)
561	3.87135 (3)	3.87468 (2)	7.80120 (5)	117.020 (2)
565	3.87151 (3)	3.87470 (3)	7.80163 (5)	117.032 (2)
569	3.87176 (2)	3.87472 (2)	7.80203 (5)	117.046 (2)
574	3.87199 (2)	3.87484 (2)	7.80252 (5)	117.064 (2)
578	3.87221 (2)	3.87485 (3)	7.80275 (5)	117.074 (2)
582	3.87245 (2)	3.87493 (2)	7.80326 (5)	117.092 (2)
587	3.87272 (2)	3.87500 (2)	7.80376 (4)	117.109 (2)
591	3.87299 (2)	3.87503 (2)	7.80403 (2)	117.123 (2)
596	3.87322 (2)	3.87508 (2)	7.80454 (2)	117.139 (2)
600	3.87344 (2)	3.87505 (2)	7.80493 (4)	117.150 (2)
604	3.87357 (3)	3.87494 (3)	7.80529 (4)	117.156 (2)
607	3.87381 (2)	3.87492 (2)	7.80555 (4)	117.167 (2)
609	3.87403 (3)	3.87490 (3)	7.80585 (4)	117.177 (2)
612	3.87421 (3)	3.87492 (3)	7.80620 (4)	117.189 (2)
614	3.87436 (3)	3.87492 (3)	7.80645 (4)	117.197 (2)
617	3.87461 (4)	3.87500 (4)	7.80676 (4)	117.212 (3)
620	3.87477 (7)	3.87497 (7)	7.80714 (4)	117.221 (5)
622	3.8748 (5)	3.8751 (5)	7.80735 (4)	117.23 (3)
625	3.87499 (3)		7.80746 (6)	117.233 (2)
629	3.87512 (2)		7.80791 (4)	117.248 (2)
634	3.87526 (2)		7.80836 (4)	117.263 (2)
638	3.87538 (2)		7.80872 (4)	117.276 (2)
642	3.87553 (2)		7.80916 (4)	117.292 (2)
647	3.87565 (2)		7.80957 (4)	117.305 (2)
655	3.87592 (2)		7.81026 (4)	117.332 (2)
664	3.87623 (2)		7.81098 (4)	117.361 (2)
672	3.87655 (3)		7.81180 (4)	117.393 (2)
689	3.87711 (2)		7.81311 (4)	117.447 (2)
Cooling				
344	3.86182 (3)	3.87115 (3)	7.78082 (9)	116.321 (3)
401	3.86434 (2)	3.87210 (2)	7.78649 (7)	116.510 (2)
430	3.86569 (2)	3.87262 (2)	7.78962 (7)	116.613 (2)
454	3.86673 (2)	3.87298 (2)	7.79193 (5)	116.690 (2)
483	3.86800 (2)	3.87346 (2)	7.79443 (5)	116.780 (2)
507	3.86906 (2)	3.87379 (2)	7.79665 (5)	116.856 (2)
516	3.86952 (2)	3.87394 (2)	7.79765 (5)	116.889 (2)
528	3.87007 (2)	3.87407 (2)	7.79863 (5)	116.924 (2)
537	3.87052 (2)	3.87424 (2)	7.79949 (5)	116.956 (2)
546	3.87088 (2)	3.87431 (2)	7.80021 (4)	116.980 (2)
555	3.87138 (2)	3.87431 (2)	7.80109 (4)	117.013 (2)
565	3.87176 (2)	3.87449 (2)	7.80189 (4)	117.040 (2)
574	3.87223 (2)	3.87460 (3)	7.80275 (4)	117.071 (2)
582	3.87267 (2)	3.87471 (2)	7.80342 (4)	117.097 (2)
587	3.87287 (2)	3.87482 (3)	7.80380 (4)	117.109 (2)
591	3.87310 (3)	3.87481 (3)	7.80421 (4)	117.122 (2)
595	3.87333 (2)	3.87483 (3)	7.80459 (4)	117.137 (2)
600	3.87359 (2)	3.87489 (2)	7.80502 (4)	117.150 (2)
602	3.87369 (2)	3.87486 (2)	7.80522 (4)	117.156 (2)
605	3.87385 (3)	3.87486 (2)	7.80549 (4)	117.167 (2)
608	3.87405 (3)	3.87492 (3)	7.80585 (4)	117.179 (2)
612	3.87431 (3)	3.87494 (3)	7.80632 (4)	117.195 (2)
622	3.87492 (2)	3.87496 (3)	7.80723 (4)	117.226 (2)
631	3.87519 (2)		7.80811 (4)	117.255 (2)
639	3.87547 (2)		7.80896 (4)	117.285 (2)
648	3.87558 (2)		7.80979 (4)	117.304 (2)
667	3.87642 (2)		7.81145 (4)	117.380 (2)

3.2. Temperature dependence of lattice parameters through high-resolution synchrotron radiation powder diffraction

Fig. 2 shows the SR-PD profile of $La_{0.68}(Ti_{0.95},Al_{0.05})O_3$ around the 004, 020 and 200 reflection peaks as a function of temperature, measured during heating, where each profile was obtained with the sample temperature kept constant. The hkl parameters were indexed on the basis of the double perovskite-type structure (Ali *et al.*, 2001, 2002). The 004 and 200 peak position decreased considerably with increasing temperature, while the 020 peak position decreased slightly. The separation of 020 and 200 peaks was large at lower temperatures, but the two peaks moved closer together with increasing temperature and eventually merged. These peaks were clearly separated up to 600 K (Fig. 2), which indicates orthorhombic symmetry. Above 600 K, it was not easy to identify whether $La_{0.68}(Ti_{0.95},Al_{0.05})O_3$ was orthorhombic or tetragonal. We analyzed the data assuming orthorhombic symmetry between 600 and 622 K (Table 2), while we assumed the tetragonal phase for data measured at above 625 K.

The lattice parameters of $La_{0.68}(Ti_{0.95}Al_{0.05})O_3$ obtained from the peak positions 004, 020 and 200 are listed in Table 2 as a function of temperature. Figs. 3, 4 and 5 show the temperature dependence of the lattice parameters, the axial ratio $b/a - 1$ and the unit-cell volume, respectively. The lattice parameters a, b and c and the unit-cell volume increased with increasing temperature (Figs. 3 and 5). The a parameter increased more rapidly than b, with the result that these two parameters became continuously closer with increasing temperature and coincided between 622 and 625 K (Fig. 3). The ratio c/a was almost independent of temperature, while b/a decreased continuously with increasing temperature and became unity between 622 and 625 K (Fig. 4).

The lattice parameters determined from data measured on heating (filled squares in Fig. 3) agree well with those determined from data measured on cooling (open squares in Fig. 3), indicating no hysteresis between heating and cooling. Similar agreements between the

Figure 2
Temperature dependence of synchrotron powder diffraction profiles for the 004, 020 and 200 reflection peaks of $La_{0.68}(Ti_{0.95},Al_{0.05})O_3$. The sample temperature was kept constant after heating.

heating and cooling data were observed for the temperature dependence of b/a and the unit-cell volume. These results strongly suggest that the orthorhombic–tetragonal phase transition is continuous and reversible. We define the order parameter, η, for the transition with respect to the axial ratio as $\eta \equiv b/a - 1$. The temperature evolution of η for a continuous phase transition can be expressed by a power law (Zhao *et al.*, 1993; Ali *et al.*, 2002) as

$$\eta \equiv b/a - 1 = A(1 - T/T_c)^{\beta}, \tag{2}$$

where T_c, T and A are the transition temperature, some temperature lower than T_c and a coefficient independent of temperature, respectively. β is the critical exponent characterizing the temperature dependence of the order parameter. For the classical approach of a mean field, $\beta = 0.5$ corresponds to a typical second-order phase transition in Landau theory. In the case of $\beta = 0.25$, the transformation is the tricritical phase transition (Zhao *et al.*, 1993). The present data from 301–622 K gave a higher critical exponent value, $\beta = 0.745\,(8) \simeq 0.75$, which indicates that the present order para-

meter decreases more continuously with temperature than that of a typical second-order phase transition. The transition temperature, T_c, of $La_{0.68}(Ti_{0.95},Al_{0.05})O_3$ was estimated to be 622.3 ± 0.6 K from (2) and the experimental data obtained in the range 301–622 K.

Because of the low resolution of laboratory X-ray powder diffraction, previous work failed to determine precisely the lattice parameters and the orthorhombic–tetragonal transition point of $La_{0.68}(Ti_{0.95},Al_{0.05})O_3$ (Yashima *et al.*, 2000; Ali *et al.*, 2001) and of $La_{2/3}TiO_{3-\delta}$ (Abe & Uchino, 1974). For example, Yashima *et al.* (2000) and Ali *et al.* (2001) estimated the transition point to be 573 K with a large uncertainty of ± 100 K. The present study has, however, succeeded in the determination of the transition point with a much higher precision of ± 0.6 K, by using the very high-resolution SR-PD technique.

4. Summary and conclusions

High-temperature SR-PD measurements of $La_{0.68}(Ti_{0.95}Al_{0.05})O_3$ were carried out to investigate precise lattice parameters as a function of temperature. It was found that this technique is more powerful than conventional laboratory-based X-ray diffraction when examining the temperature dependence of lattice parameters around the transition temperature. A phase transition from orthorhombic to tetragonal symmetry was observed, and the transition temperature was determined to be 622.3 ± 0.6 K. The a and c parameters increased considerably faster with increasing temperature than b, with the result that the values of a and b became closer with increasing temperature and coincided between 622 and 625 K. Thus, with increasing temperature, the ratio b/a decreased continuously and became unity at the orthorhombic–tetragonal phase-transition point. Good agreement was observed for the lattice parameters and the axial ratios b/a determined from the data measured on heating and on cooling. These results strongly suggest that the transition is continuous and reversible. The critical exponent for the b/a curve was calculated as $\beta = 0.75$, which suggests that the phase transition was more continuous than a typical second-order phase transition.

Figure 3
Temperature dependence of the lattice parameters of $La_{0.68}(Ti_{0.95},Al_{0.05})O_3$. Filled and open squares denote data measured on heating and cooling, respectively.
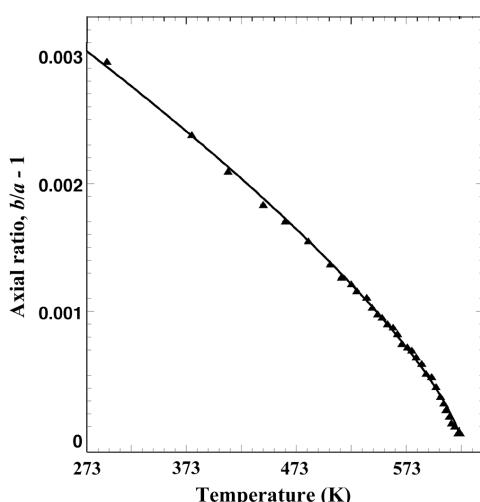

Figure 4
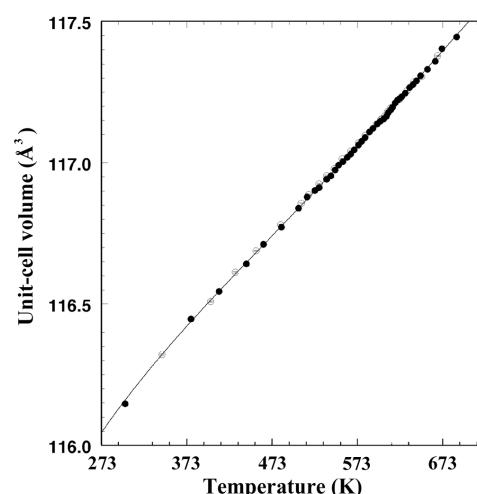Temperature dependence of the axial ratio, b/a, of $La_{0.68}(Ti_{0.95},Al_{0.05})O_3$. The solid line was obtained assuming a power law, (2).

Figure 5
Temperature dependence of the unit-cell volume of $La_{0.68}(Ti_{0.95},Al_{0.05})O_3$. Filled and open circles indicate data obtained on heating and cooling, respectively.

References

Abe, M. & Uchino, K. (1974). *Mater. Res. Bull.* **9**, 147–156.

Ali, R., Yashima, M., Tanaka, M., Yoshioka, H., Mori, T. & Sasaki, S. (2002). *J. Solid State Chem.* **164**, 51–59.

Ali, R., Yashima, M., Yoshimura, M. & Yoshioka, H. (2001). *J. Am. Ceram. Soc.* **84**, 468–470.

Hart, M., Cernik, R. J., Parrish, W. & Toraya, H. (1990). *J. Appl. Cryst.* **23**, 286–291.

Kawasaki, K., Takagi, Y., Nose, K., Morikawa, H., Yamazaki, S., Kikuchi, T. & Sasaki, S. (1992). *Rev. Sci. Instrum.* **63**, 1023–1026.

Kim, I. S., Nakamura, T., Inaguma, Y. & Itoh, M. (1994). *J. Solid State Chem.* **113**, 281–288.

MacEachern, M. J., Dabkowska, H., Garrett, J. D., Amow, G., Gong, W., Liu, G. & Greedan, J. E. (1994). *Chem. Mater.* **6**, 2092–2102.

Sasaki, S., Mori, T., Mikuni, A. & Iwasaki, H. (1992). *Rev. Sci. Instrum.* **63**, 1046–1050.

Skapin, S., Kolar, D. & Suvorov, D. (1993). *J. Am. Ceram. Soc.* **76**, 2359–2362.

Stephens, P. W., Cox, D. E. & Fitch, A. N. (2002). *Structure Determination From Powder Diffraction Data*, edited by W. I. F. David, K. Shankland, L. B. McCusker & Ch. Baerlocher, p. 49. Oxford University Press.

Suvorov, D., Valant, M., Skapin, S. & Dolar, D. (1998). *J. Mater. Sci.* **33**, 85–89.

Tanaka, M. (2000). Photon Factory Activity Report 199 #17, KEK Progress Report 2000–1, edited by Y. Murakami, H. Adachi, Y. Hori, K. Ito, A. Kobayashi, K. Mase, F. Mori, K. Ohsumi, H. Sugiyama & M. Suzuki, pp. 42–44. High Energy Acceleration Research Organization, Tsukuba, Japan.

Toraya, H. (1986). *J. Appl. Cryst.* **19**, 440–447.

Yashima, M., Ali, R., Tanaka, M., Mori, T. & Sasaki, S. (2001). *J. Rock Mineral. Soc. Jpn*, **30**, 74–75.

Yashima, M., Ali, R. & Yoshioka, H. (2000). *Solid State Ionics*, **128**, 105–110.

Yashima, M., Sasaki, S., Yamaguchi, Y., Kakihana, M., Yoshimura, M. & Mori, T. (1998). *Appl. Phys. Lett.* **72**, 182–184.

Yokoyama, M., Ota, T. & Yamai, I. (1989). *J. Crystal Growth*, **96**, 490–496.

Yoshioka, H. (1994). *Jpn. J. Appl. Phys.* **33**, L945–L948.

Yoshioka, H. (2002). *J. Am. Ceram. Soc.* **85**, 1339–1341.

Yoshioka, H. & Kikkawa, S. (1998). *J. Mater. Chem.* **8**, 1821–1826.

Zhao, Y., Weidner, D. J., Parize, J. B. & Cox, D. E. (1993). *Phys. Earth Planet. Int.* **76**, 17–34.